A PHASE SPACE ANALYSIS OF BAROCLINIC FLOW

Doyne FARMER
Center for Nonlinear Studies, MS B258, Los Alamos National Laboratory, Los Alamos, NM 87545, USA

and

John HART and Patrick WEIDMAN
University of Colorado, Boulder, CO, USA

Received 27 May 1982

The qualitative dynamics of a baroclinic flow experiment are studied by constructing phase space coordinates from a single time series. As the stress on the flow is increased we observe steady, periodic, quasiperiodic, and chaotic flow. The chaotic attractor we observe near the transition has the appearance of a thickened torus.

In this paper we investigate waves produced by baroclinic instability [1,2]. The apparatus consists of a rotating cylindrical container filled with two immiscible fluids of different density. A rigid contact lid corotates at an angular speed ω slightly greater than the basic cylinder speed Ω. For low values of ω the interface is static, but above a critical value waves appear on the interface, and we successively observe periodic, quasiperiodic, and chaotic flow. This bifurcation sequence is similar to that previously observed for Taylor–Couette flow [3].

The physical quantity we measure is the height of the interface between the two fluids. This is done using a thin vertical wire spanning the interface. Since the two fluids have different conductivities, motions of the interface cause changes in the impedance of the wire. These measurements produce a single time series $x(t)$, which represents only one of the (in principle) infinite degrees of freedom available for the fluid's motion. Thus, in the phase space of this flow we are observing motion along only one dimension. As has been shown in refs. [4–6], however, qualitative behavior in other dimensions can be recovered from $x(t)$ by any of several methods. The first method we employ here constructs three phase space coordinates (x_1, x_2, x_3) using time delays. We take $x_1(t) = x(t)$, $x_2(t) = x(t - \tau_1)$ and $x_3(t) = x(t - \tau_2)$. Although the representation of the system's attractors obtained in this manner is not unique, we find that other choices of coordinates give qualitatively similar pictures.

The relevant physical parameters for all experiments reported here are the quiescent depth of each layer $H = 7.0$ cm, the cylinder diameter $L = 11.5$ cm, its angular velocity $\Omega = 3.38$ rad/s, and the average kinematic viscosity of the two fluids, $\nu = 0.014$ cm^2/s. In each experiment we vary the normalized differential spin rate (Rossby number) $R_0 = \omega/2\Omega$ while holding the Froude number $F = 4\Omega^2 L^2 \rho/(gH\Delta\rho)$ constant. A summary of our measurements is given in fig. 1. The cases we analyze in detail in figs. 2 and 3 both have $\Delta\rho/\rho = 0.052$.

In fig. 2 $R_0 = 0.169$. The time series $x(t)$ is given in fig. 2a, and fig. 2b is the power spectrum of $x(t)$. A plot of x_1 versus x_2 (fig. 2c) suggests that the underlying attractor of this flow is a two dimensional torus, i.e., quasiperiodic flow containing two irrationally related frequencies. This is more clearly demonstrated in the Poincaré section of fig. 1d, made by plotting x_2 versus x_3 whenever $x_1 = 0$ (the average value). The resulting cross section or "slice" is the intersection of the attractor and a plane, and forms two closed curves, one for trajectories coming out of the plane and the other for trajectories going into the plane. Each of these closed curves is topologically equivalent to a circle.

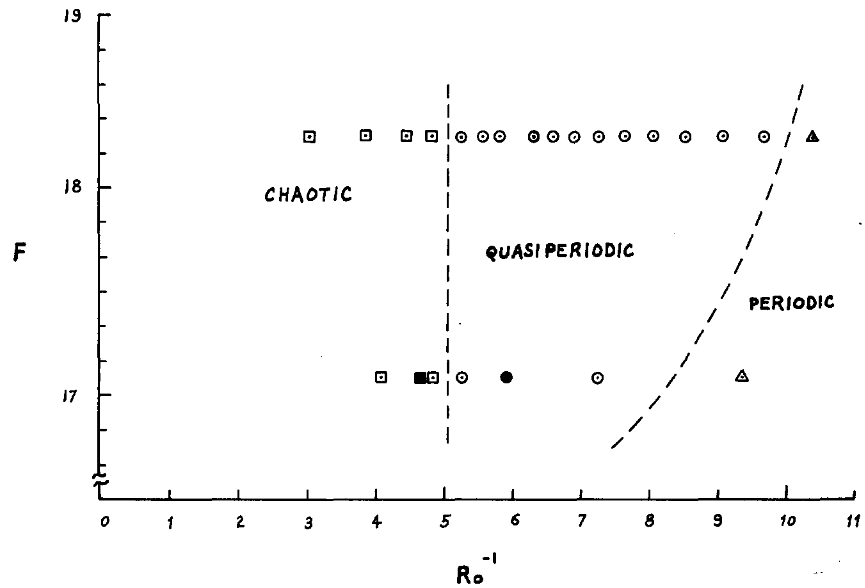

Fig. 1. Summary of experiments. The experiments at parameter values marked in black are presented in detail in figs. 2 and 3. $F = 4\Omega^2 L^2 \rho/(gH\Delta\rho)$ is the Froude number, and $R_0 = \omega/2\Omega$ is the Rossby number.

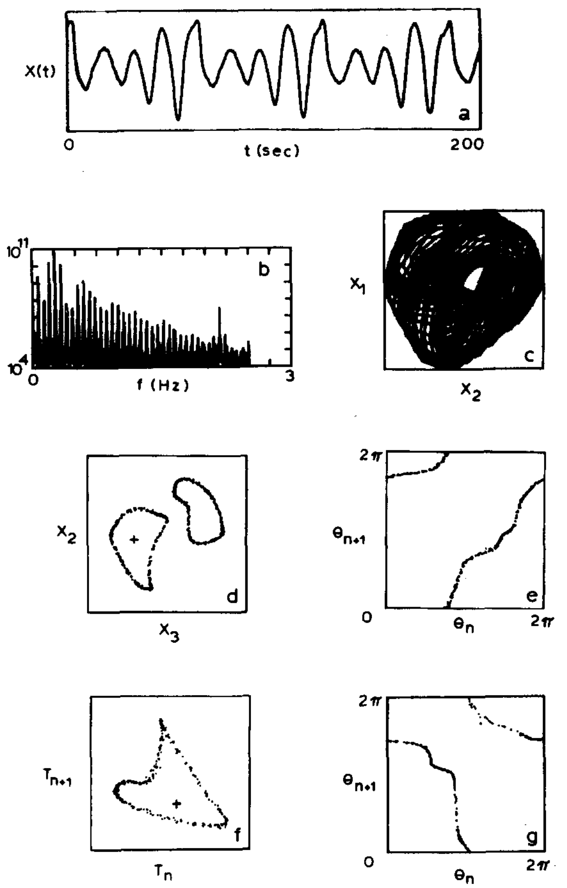

Fig. 2. Quasiperiodic flow, $R_0 = 0.169$. (a) A 200 s sample of the time series $x(t)$. Note that $x(t)$ was low pass filtered at 3 Hz. (b) A power spectrum of $x(t)$. To construct the spectrum $x(t)$ was sampled at an interval $\Delta t = 0.8$ s and divided into ten 4096 point records. After smoothing with a cosine bell, the FFT of each record is squared and averaged together. (c) A reconstructed phase plot, $x(t)$ versus $x(t-\tau)$, with $\tau = 7.8$ s. (d) A Poincaré section, constructed by plotting $x(t-\tau_1)$ versus $x(t-\tau_2)$ whenever $x(t) = 0$. $\tau_1 = 7.8$, and $\tau_2 = 15.6$. (e) Return map for left section of (d). The cross is the reference point used to calculate θ_n. (f) Plotting successive periods between upward zero crossings of $x(t)$ gives an alternative representation of the Poincaré section. (g) A return map constructed from (f).

The dynamics on the torus can be summarized by the construction of a one dimensional map of the circle onto itself. To do this, as each successive point appears on the left hand Poincaré section it is assigned an angle θ_n relative to the interior reference point shown in fig. 2d. A plot of θ_{n+1} versus θ_n, shown in fig. 2e, illustrates how the circle maps onto itself. Notice that although this map is one to one, as it must be for a torus, on the right hand side it is developing an inflection point, as it must to make a transition to chaos.

In order to demonstrate the independence of the qualitative behavior on the choice of phase coordinates, in figs. 2f and 2g a Poincaré section and return

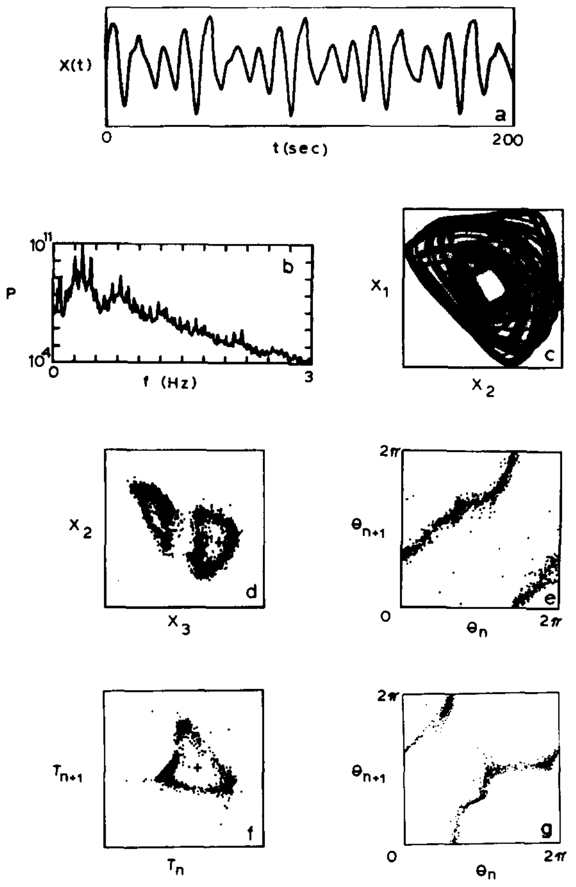

Fig. 3. Chaotic flow. Same as fig. 2, except that R_0 = 0.224, $\tau = \tau_1$ = 3.3, τ_2 = 6.6, and Δt = 0.22.

map are made by an alternate method. Fig. 2f is a plot of T_{n+1} versus T_n, where T_n is the time between successive upward zero crossings of $x(t)$. Note the similarity to fig. 2d. In fig. 2g a return map is constructed from fig. 2f by again plotting successive angles relative to the plotted central reference point. The development of the inflection point is even more pronounced in this representation.

Fig. 3 shows the corresponding set of pictures when R_0 = 0.224. The power spectrum (fig. 3b) contains broadband components, implying that the flow is now chaotic. The Poincaré sections indicate that the torus is now "thick" or "fuzzy". Apparently the chaotic motion is largely transverse to the persistent quasiperiodic motion. At this level of resolution we see no indications of fractal structure, and we are unable to determine whether or not the dimension of the attractor is less than three. As R_0 increases, the amplitude of the chaotic motion increases, until at R_0 = 0.30 the amplitude of chaotic motion becomes comparable to that of quasiperiodic motion, and the torus is destroyed; the Poincaré sections for this case have the appearance of scatter plots.

Other than the qualitative statements above, we are unable at this stage to say very much about the nature of this chaotic attractor. Our results indicate, though, that the transition to chaos proceeds through the development of an inflection point in a mapping of the circle. Because of the potential universal properties of this transition [7], there is currently a great deal of interest in transitions of this type. Some similarities in phenomenology are apparent in a mapping due to Curry and Yorke [8], in numerical studies of a seven mode truncation of the Navier–Stokes equations by Franceschini [9], and in numerical studies of the dissipative nonlinear Schrödinger equation by Huerre, Moon, and Redekopp [10]. We plan to explore the possible connections by making a detailed study of the transition region.

The use of phase space coordinates gives a clear picture of a torus underlying a quasiperiodic flow, and illustrates some qualitative features of the transition that would not be clear otherwise. Beyond the inception of chaotic motion at a critical value of the control parameter, the amplitude of chaotic motion increases relative to that of quasiperiodic motion, until the underlying torus is destroyed.

References

[1] J. Hart, J. Atmos. Sci. 30 (1973) 1017.
[2] J. Hart, J. Atmos. Sci. 33 (1976) 1874.
[3] P.R. Fenstermacher, H.L. Swinney and J.P. Gollub, J. Fluid Mech. 94 (1979) 103.
[4] N. Packard, J. Crutchfield, D. Farmer and R. Shaw, Phys. Rev. Lett. 45 (1980) 712.
[5] H. Froehling, J. Crutchfield, D. Farmer, N. Packard and R. Shaw, Physica 3D (1981) 605.
[6] F. Takens, Detecting strange attractors in turbulence, preprint.
[7] S. Shenker, Scaling behavior in a map of a circle onto itself: empirical results, Univ. of Chicago, preprint.
[8] J. Curry and J. Yorke, The structure of attractors in dynamical systems (Springer, Berlin, 1978) p. 48.
[9] V. Franceschini, private communication.
[10] P. Huerre, private communication.